19th International Conference on
Adaptive Structures and Technologies
October 6-9, 2008
Ascona, Switzerland

Active Trailing-edge Flap Blades Utilizing Piezoelectric Buckling Actuators

Jae-Sang Park[1]*, Sung-Nam Jung[2], Yung-Hoon Yu[3] and Young-Hyun You[4]
Dept. of Aerospace Information Engineering, Konkuk University, Hwayang-dong, Gwangjin-gu,
Seoul 143-701, KOREA
[1]Tel.: 82-2-458-1901, Fax.:82-2-2049-6098, E-mail:smartrotor@gmail.com

ABSTRACT

This paper presents the preliminary design and analysis studies of the piezoelectric buckling beam actuators for Active Trailing-edge Flap (ATF) blades and conducts the vibratory loads reduction analysis of the ATF blade using piezoelectric buckling beam actuators. Two piezoelectric stack actuators are used to buckle the beam both upward and downward directions, as a result the trailing-edge flap can be deflected both upward and downward directions. The numerical studies based on finite element method show the actuation performance of the actuator and gives the required voltage to get the target flap deflection angle. For the vibratory loads reduction analysis of the ATF blade using piezoelectric buckling beam actuators, a multibody dynamic analysis modeling is introduced. The prescribed moment based on Individual Blade Control (IBC) is applied to the flap hinge for the controls of the flap motion. The numerical results show the vibratory loads of the ATF blade at the fixed- and rotating-systems. The loads reduction results indicate that the ATF blade using piezoelectric buckling beam actuators reduces the vibratory loads siginificantly although relatively lower input-voltage is applied to actuators.

Keywords: Piezoelectric buckling beam actuators, Active Trailing-edge Flap blades, and Vibratory loads reduction analysis

1. INTRODUCTION

In order to reduce the vibratory loads of rotorcrafts, during the last two decades, active control methodologies to modify directly the periodic aerodynamic loads acting upon the rotor blades have been examined. The most representative scheme is Active Trailing-edge Flap (ATF) blade using piezoelectric actuators as shown in Figure 1.

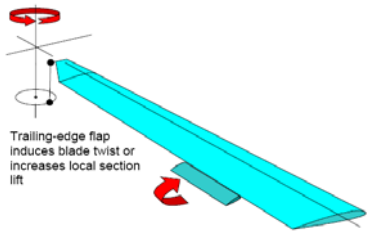

Figure 1 Active Trailing-edge Flap (ATF) blade

The ATF blade uses a small flap on each blade to generate the desired unsteady aerodynamic

loads. This scheme is effective, but uses less power than the conventional Individual Blade Control (IBC) techniques. In ATF techniques, a partial span trailing-edge flap is located at the outboard region of the blade.

The numerical and experimental researches on the ATF rotor blade have been extensively conducted [1, 2]. Their results showed the potential of the ATF blade to significantly reduce the vibratory loads, alleviate noise, and enhance the rotor performance and handling qualities.

With researches on the ATF blades, over the past decade, various piezoelectric actuators in order to deflect a trailing-edge flap of a rotor blade have been developed. There are piezoelectric bender actuator [3], piezoelectric tube actuator [4] and piezoelectric stack actuators [5, 6]. Among them, the actuators based on piezoelectric-stack actuators have been widely applied to the ATF blade. However, they can only produce a relatively small displacement. Therefore it should be amplified in order to achieve a required flap deflection. This limitation needs the complex amplification mechanisms such as a double lever mechanism [5] or X-frame mechanism [6].

These amplification mechanisms result in the weight increase of the blade and complexity. Thus, to solve this problem, recently the piezoelectric buckling actuator was developed [7]. As shown in Figure 2, the piezoelectric stack actuator produces the free elongation strain, which causes the buckling of the beam at the buckling load. As a result, the large rotation of the output shaft is obtained. This concept can be used to deflect the trailing-edge flap of the rotor blade without any complex amplification mechanism. Thus, the piezoelectric buckling actuator is very simple, compact and lightweight for deflection of the trailing-edge flap.

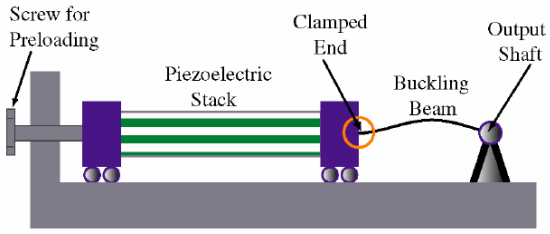

Figure 2 Concept of the piezoelectric buckling beam actuator [7]

Therefore, in this work, the piezoelectric buckling beam actuator to control the trailing-edge flap is proposed and its design and performance analysis are conducted. Furthermore, the aeroelastic analysis of the ATF blade utilizing the piezoelectric buckling beam actuators is conducted. For the numerical analysis, a multibody dynamic model for the ATF blade is studied. Through IBC scheme, the most effective actuation frequency and control phase angle for reduction of vibratory loads at the hub are determined. Also, the loads on the blade such as flap bending moments and torsional moments are predicted. Through the vibratory loads reduction analysis, the efficiency of the present ATF blade in vibratory loads reduction is investigated.

2. Modeling and analysis of piezoelectric buckling beam actuator for ATF blade

2-1. Modeling of piezoelectric buckling beam actuator

When a beam is buckled, the beam may be deflected upward or downward direction. Although a large rotation at the edges is obtained from the beam buckling, it is difficult to control the direction of the buckling deflection when the ideal column under perfect loads is considered.

However, it is important to control the buckling deflection direction since the trailing-edge flap should be deflected both upward and downward.

Therefore, in this study, in order to control the buckling deflection direction, the eccentric loads with geometric offset are considered. As shown in Figure 3, when the upper eccentric load is applied to the beam, the beam will be deflected downward. Similarly, when the lower eccentric load is considered, the beam may be deflected upward. To apply two types of eccentric loads to the beam, two piezoelectric stack actuators are used as given in Figure 4. To consider eccentric offset, the beam base which is thicker than the buckling beam is used.

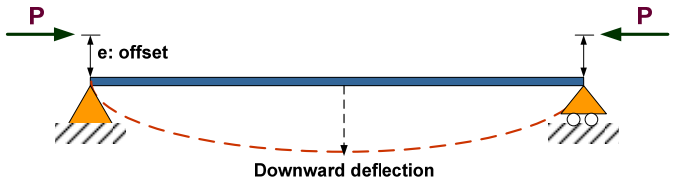

Figure 3 Buckling beam under eccentric load

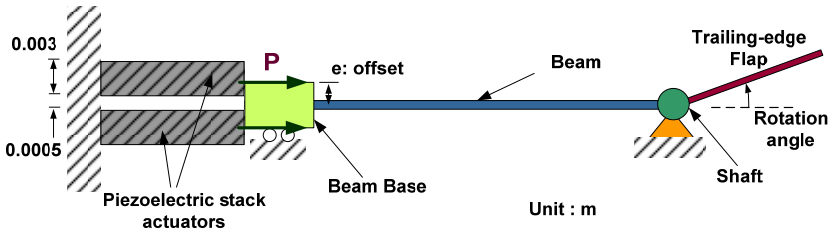

Figure 4 Piezoelectric buckling beam actuator for ATF

If the input-voltage is applied to the only upper piezoelectric stack actuator, the upper eccentric load is applied to the beam structure. The upper eccentric load deflects the beam downward and then, the flap is deflected upward. To the contrary, when the input-voltage is applied to the only lower piezoelectric stack actuator, the lower eccentric load is obtained. The lower eccentric load buckles the beam upward and then, the flap is deflected downward.

2-2. Design requirement for actuator

The most important design requirement for the piezoelectric buckling beam actuator is the flap hinge moment. In general, in order to reduce the vibratory loads of rotorcrafts significantly, the flap deflection of $\pm 4^\circ$ is required. Therefore, there is a hinge moment at the flap hinge to sustain the desired flap deflection angle and the actuator should overcome the flap hinge moment.

In this paper, the only aerodynamic hinge moment is considered and it is assumed that the hinge moments due to centrifugal and inertia effects can be neglected. The flap hinge moment due to the aerodynamic effect on the flap is predicted from Equation (1) which is derived from assumptions [5]; blade element theory/momentum theory in hover, uniform inflow mode and untwisted blade.

$$H = \frac{1}{2}\rho\Omega^2 c_f^2 \left[\left(\frac{R_2^3}{3} - \frac{R_1^3}{3} \right) \left\{ C_{l_\alpha} \frac{dC_h}{dC_l} \left(\theta_0 + \frac{\Delta\alpha_0}{\Delta\delta}\delta \right) + \frac{dC_h}{d\delta}\delta \right\} - C_{l_\alpha} \lambda R_{tip} \left(\frac{R_2^2}{2} - \frac{R_1^2}{2} \right) \frac{dC_h}{dC_l} \right] \quad (1)$$

When the following condition as give in Table 1 is considered, the predicted flap hinge moment is 0.041 N-m.

Table 1. The properties of blade and flap for prediction of flap hinge moment

· Blade radius R	1.397m
· Flap length $R_f=R_2-R_1$	0.20R
· Flap location	0.75R
· Blade chord length c	0.1175m
· Flap chord length c_f	0.15c
· Airfoil	NACA0012
· Rotation speed	687.5 RPM
· Test medium density	2.4319 kg/m^3

2-3. Actuation performance of piezoelectric buckling beam actuator

For the numerical analysis of the buckling beam actuator, finite element method using is used. The buckling beam structure is modeled through the first-order shear deformation plate theory. 12x2 mesh with 4 node isoparametric elements is used. The von Karman nonlinear strain- displacement relationship and Newton-Rapson method are used to investigate the postbuckling behavior of the beam under eccentric loads. The piezoelectric buckling beam actuator consists of piezoelectric stack actuators and beam structure. In this example, PZT-5A stack is used for the piezoelectric stack actuator with 10 layers. For the beam structure, to reduce the blade weight, S-glass composite material is selected.

Figure 5 shows the finite element model for a buckling beam structure. Its dimension in xy plane is 0.0475x0.005 m. The boundary condition at the input side where the piezoelectric compressive loads are applied is considered as clamped or simply supported. The other side for the flap shaft is modeled as a simply supported boundary condition.

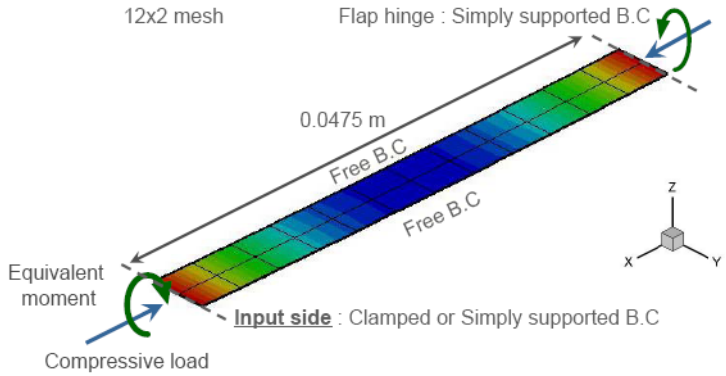

Figure 5 Finite element model for buckling beam structure

Figure 6 presentes the effect of boundary condition at input side on the actuation performance. As one can see, when the input-voltage is low, both clamped and simply supported conditions produce the similar flap rotation angle. However, the input-voltage is increased, the clamped condition produces larger flap rotation angle than the simply supported condition does. Therefore, in this paper, the clamped boundary condition at the input side is used for a baseline model.

The effect of the eccentric offset on the flap rotation angle is given in Figure 7. For the baseline model, the nominal offset of 0.00175 m is used. As the offset is decreased, the flap rotation angle is decreased. In addition, when the offeset goes to zero, the bifurcation buckling behavior is observed. As shown in this figure, the magnitude of the offset has a significant influence on the actuation performance.

Figure 8 shows the relationship between the applied moment to the flap hinge and the flap

rotation angle with different eccentric offsets. From this figure, for the nominal offset, to get the target angle (4 deg.), the moment of approximately 0.017 N-m is required. However, this value is much lower than the required hinge moment of 0.041 N-m from the design requirement. This is because this actuation performance analysis does not consider the aerodynamic effects on the flap.

The relationship between the input-voltage and the applied moment at the hinge is shown in Figure 9. To produce the target moment of 0.041 N-m from the design requirement, about 38 volt should be applied to a PZT-5A stack. Figures 8 and 9 give that the piezoelectric buckling beam actuator can produce the target hinge moment to sustain the desired flap deflection angle.

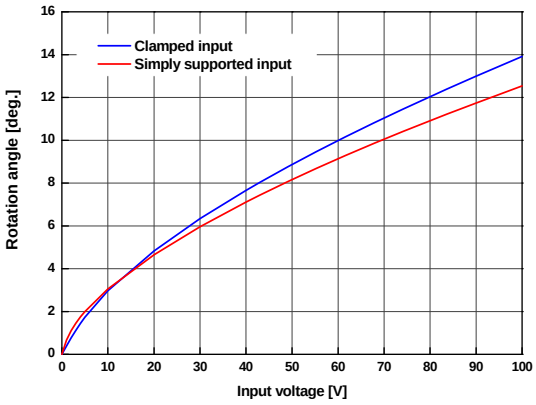

Figure 6 Effect of boundary condition at input side on the actuation performance

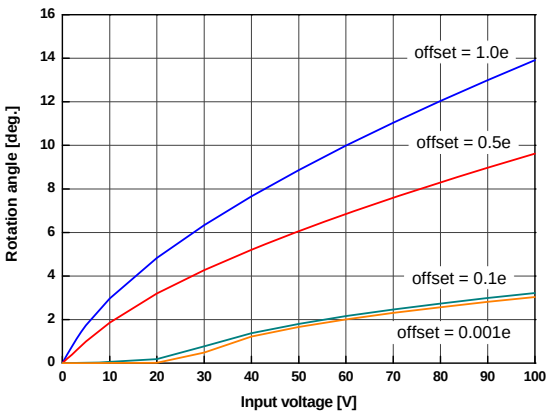

Figure 7 Effect of eccentric offset on the actuation performance

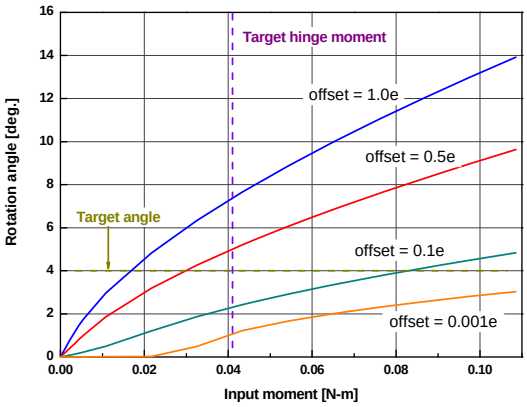

Figure 8 Relationship between the input moment and the flap rotation angle

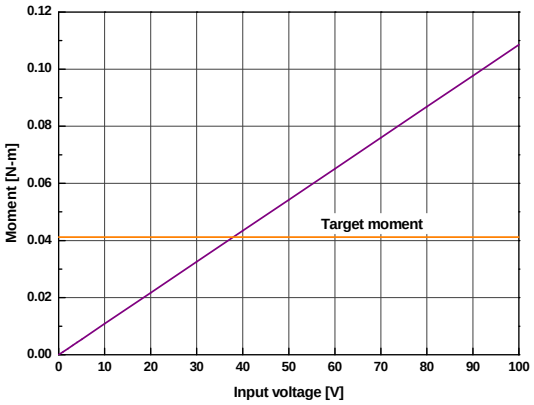

Figure 9 Relationship between the input voltage and the applied moment at the flap hinge

3. Aeroelastic analysis of the ATF blade utilizing piezoelectric buckling beam actuators

3-1. Multibody dynamic modeling of ATF blades

For a multibody dynamic modeling of ATF blade, DYMORE [8] which is a nonlinear flexible multibody dynamics analysis tool is used. DYMORE uses Dr. Hodges' the geometrically exact beam theory [9] for the beam elastic model and Peters and He's finite state dynamic inflow model [10] for the aerodynamic model. In addition, the autopilot theory is used for the trim analysis.

The present scaled ATF blade model is based on the NASA extension-twisting coupled blade [11] which is the baseline blade for NASA/Army/MIT Active Twist Rotor (ATR) blade [12]. Its blade properties are given in Table 2. Furthermore, in this study, the flap is assumed to be 20% of the blade span and 15% of the chord, located at 75% of the blade radius. The sectional properties of the flap are assumed to be 15% of the main blade properties.

Table 2 The properties of the baseline blade for the ATF

· Rotor type	Fully articulated	· Pitch axis	25% c
· Number of blades, b	4	· Elastic axis	25% c
· Blade chord, c	0.1175 m	· Center of gravity	25% c
· Blade radius, R	1.397 m	· Rotor rotational speed Ω	687.5 RPM
· Solidity, $bc/\pi R$	0.0982	· Axial stiffness	$2.0\text{x}10^{6}$ N
· Lock number	9.0	· Torsional stiffness	$4.847\text{x}10^{1}$ N-m^2
· Airfoil	NACA0012	· Flapwise bending stiffness	$4.331\text{x}10^{1}$ N-m^2
· Blade pretwist	-10 deg.	· Chordwise bending stiffness	$7.026\text{x}10^{3}$ N-m^2
· Hinge offset	0.0762 m	· Mass per unit length	0.696 kg/m
· Root cutout	0.3175 m	· Torsional inertia per unit length	$3.747\text{x}10^{-4}$ kgm^2/m

Figure 10 shows a multibody model of the present ATF blade in this paper. The hub is modeled as a rigid body, and connected with a revolute joint underneath. It is under a prescribed rotation with nominal rotating speed Ω. Root retention is a passive elastic beam rigidly attached to the hub, and the reaction loads at the attachment point are extracted and added over four of them to give the hub vibratory loads. Because the ATF rotor is a fully articulated system, three revolute joints are consecutively located between the root retention and the active blade to represent flap, lead-lag, and feathering hinges. In the present model, the flapping and lead-lag hinges are coincident. Active blades are attached to represent the ATF blades, and they can be divided into 3 regions: the passive inner blade (blade segment 1), active flap blade (blade segment 2), and passive outer blade (blade segment 3) region. Each blade region is discretized during the analysis at least by three beam elements per blade, each with the 3rd-order interpolation polynomials.

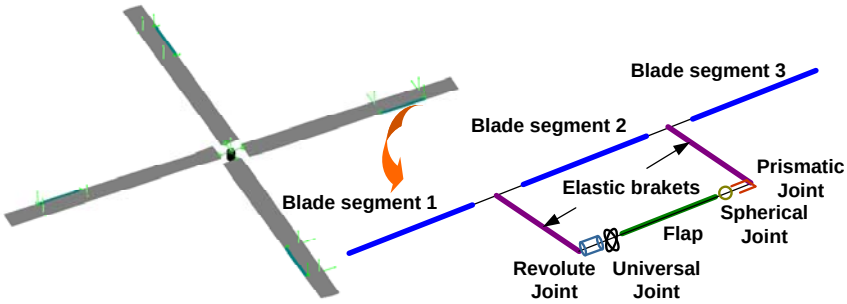

Figure 10 Multibody model for the ATF blade

Finally, to represent the trailing-edge flap in DYMORE, as shown in Figure 10, several rigid/elastic joints for hinges and elastic beams for the brackets and flap are used. In the actual system, the sequential actuation of upper and lower PZT stack actuators deflects the flap upward and downward sequentially. Instead of the multibody modeling for the piezoelectric buckling beam actuator inside flap, in this study, the flap motion is described as a prescribed equivalent moment at the flap hinge. The equivalent moment considering sine-dwell signal with control phase variation which describes IBC scheme as give in Figure 11 is applied to the hinge. The magnitude of moment applied to the hinge is assumed to be 0.045 N-m, which requires input-voltage of approximately 42 volts to each PZT-5A stack actuator.

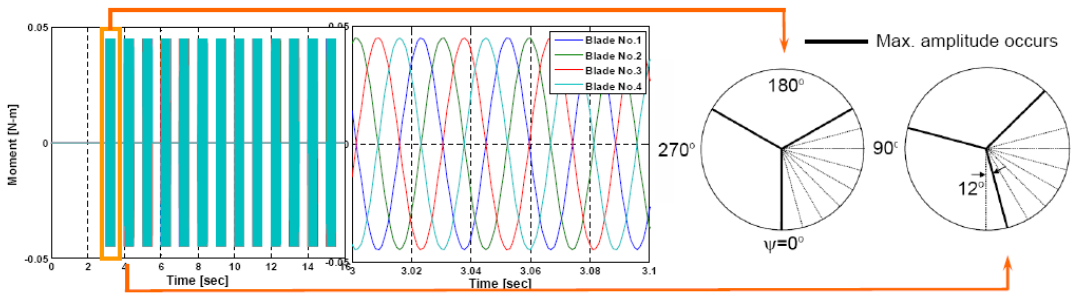

Figure 11 Example of prescribed input moment for an IBC mode considering 3/rev actuation with 12 divisions of control phase angle

3-2. Vibratory loads reduction analysis

3-2-1 Trim analysis

Before the vibratory loads reduction analysis, the trim analysis is conducted for following forward flight condition; the advance ratio $\mu = 0.140$ and rotor shaft angle of attack $\alpha_s = -1°$. The target thrust is 1000 N, target pitching and rolling moments are both 0 N-m. Figure 12 shows the results of the trim analysis. Figure 12(a) indicates that the trim analysis is completed successfully. From the trim analysis, the trimmed three pitch control angles - collective, lateral cyclic and longitudinal cyclic pitch angles - are obtained as given in Figure 12(b).

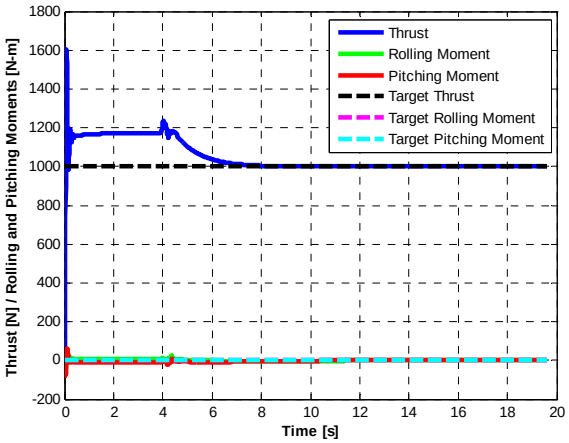

Figure 12(a) Trim analysis results

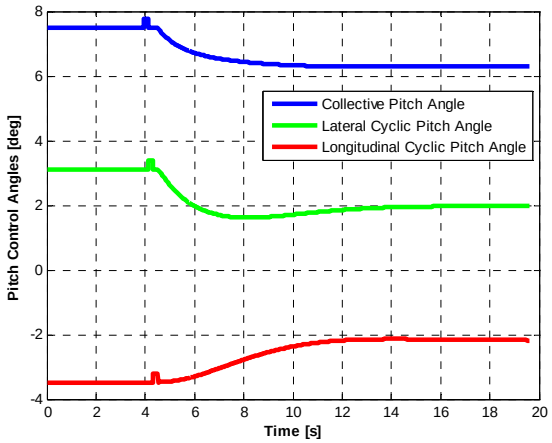

Figure 12(b) Trimmed pitch control angles

3-2-2 Vibratory loads reduction analysis at the hub

After the trim analysis is completed, first the vibratory loads at the hub are predicted. Figure 13 shows the time history of hub vertical shear forces when the 3/rev actuation frequency is applied to the flap. As one can see, the vibratory loads magnitude is changed considerably for certain control phase actuation. The biggest reduction is observed for 11 to 11.5s. Through conversion from time domain results to frequency domain, the 4/rev hub shear vibratory load component is predicted since the 4/rev loads component is the most dominant component for the four-bladed rotor system in general.

Figure 14 gives the variation of the 4/rev hub shear vibratory loads when 3,4 and 5/rev actuation frequency with the control phase angle is applied to the flap actuation. As one can see, the hub vertical shear load component is reduced by approximately 93% when the 3/rev actuation frequency with 243° control phase angle is applied. This reduction result of the present ATF blade is

comparable with that of the other active rotor control systems, although much lower input-voltage (42 volts) is applied to the ATF blade. It is known that the previous ATF blades require the input voltage of 100~500 volts generally. For the hub forward shear load component, the 3/rev actuation frequency is also the most effective when 290° control phase is considered and it can reduce the hub forward shear load component by 46%.

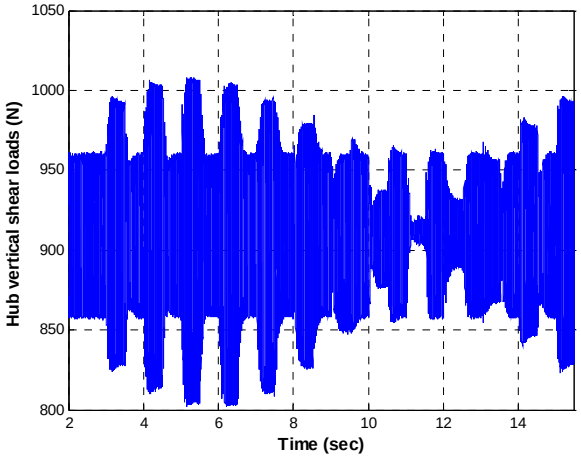

Figure 13 Time history of hub vertical shear loads with 3/rev actuation frequency

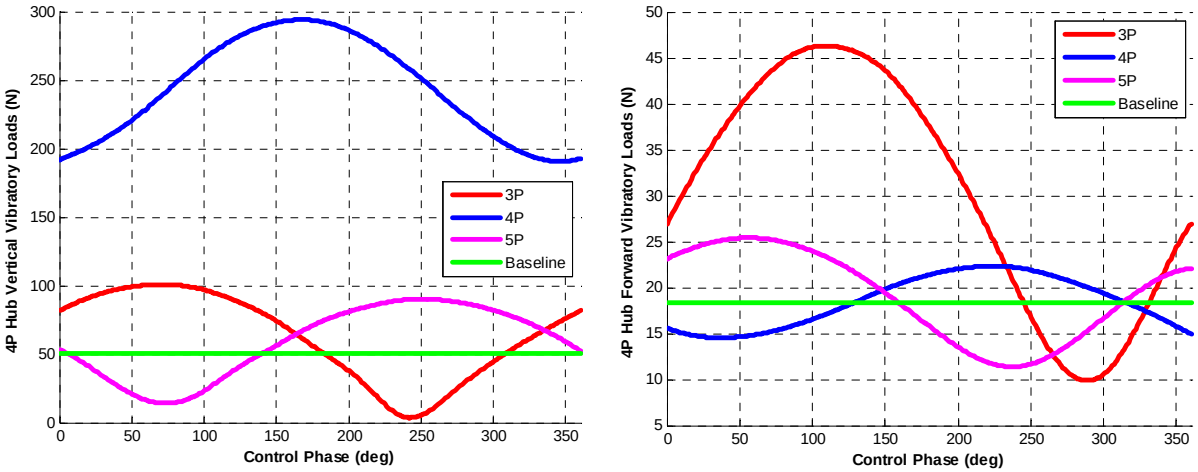

(a) Vertical component **(b) Forward component**

Figure 14 Variation of 4/rev hub shear vibratory loads

3-2-3 Vibratory loads reduction analysis at the blade

Following the vibratory loads reduction analysis at the hub, the rotating-system loads such as the flap bending moment and the torisonal moment of the blade are predicted. Unlike the previous fixed-system loads prediction, there are 3,4, and 5/rev frequency components in the rotating-system loads. The 3,4, and 5/rev frequency load components of the flap bending moment at 28.7% span location are shown in Figure 15. As one can see, for all frequency load components, the flap bending moments can be reduced significantly. Figure 16 shows the 3, 4, and 5/rev frequency load components of the torsional moment at 33.6% span location. On the contrary to the previous results of bending moments, the torsional moments are increased significantly. The *N*/rev actuation frequency (*N*=3, 4, and 5) increases the *N*/rev frequency torsional moment, respectively. Therefore, a special attention is required since it may affect the blade structural integrity.

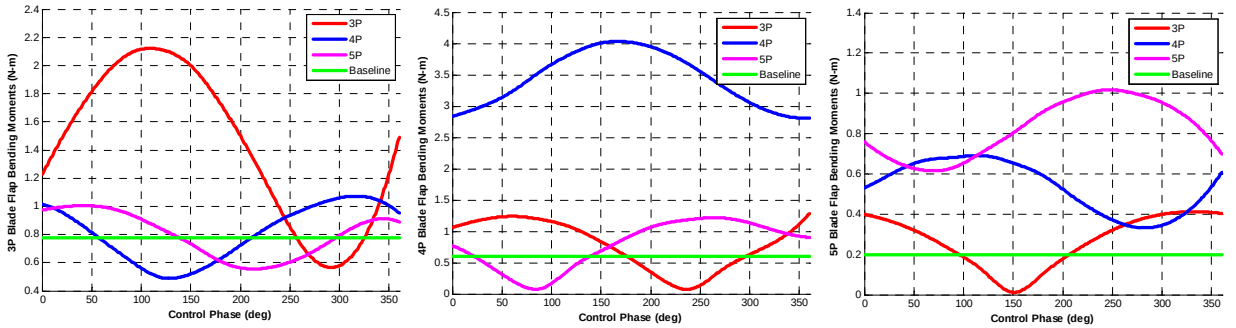

(a) 3/rev frequency component **(b) 4/rev frequency component** **(c) 5/rev frequency component**

Figure 15 Variation of blade flap bending moments at 28.7% span location

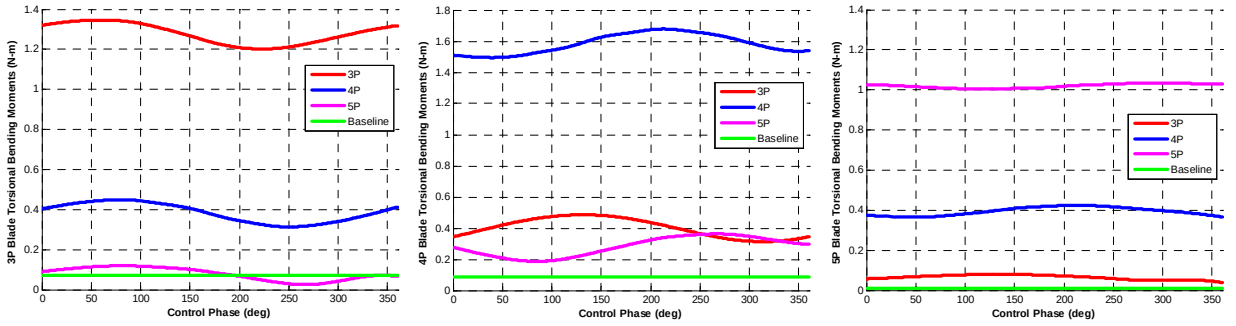

(a) 3/rev frequency component **(b) 4/rev frequency component** **(c) 5/rev frequency component**

Figure 16 Variation of blade torsional moments at 33.6% span location

4. CONCLUSIONS

This paper presents the vibratory loads reduction analysis of the ATF blade using the piezoelectric buckling beam actuator. First, the preliminary design and actuation performance analysis of the piezoelectric buckling beam actuator are conducted for the application to the trailing-edge flap control. The present piezoelectric buckling beam actuator uses two PZT-5A stacks in order to deflect the flap both upward and downward. The numerical studies based on finite element methods show that the designed buckling beam actuator can produce the target hinge moment to sustain the desired flap deflection angle although relatively low input-voltage is applied to each PZT-5A stack. Second, a multibody model for the ATF blade is constructed for the aeroelastic analysis. The flap is modeled as various rigid/elastic joints and elastic beams. The trailing-edge flap motion is described as a prescribed equivalent moment at the flap hinge. The vibratory loads reduction analyses at the hub and the blade show that the present ATF blade reduce vibratory loads significantly although much lower input-voltage is applied to actuators.

ACKNOWLEDGEMENTS

This work was supported by Brain Korea 21 in 2008 and the Korea Foundation for International Cooperation of Science & Technology(KICOS) through a grant provided by the Korean Ministry of Education, Science & Technology(MEST) in 2008 (No. K20601000001).

REFERENCES

1. Milgram, J. H., and Chopra, I., “Helicopter Vibration Reduction with Trailing-Edge Flaps,” 36th AIAA/ASME/ASCE/AHS/ASC Structures, Structural Dynamics and Materials Conference, New Orleans LA, April 1995.Lee, C. K. and F. C. Moon, “Modal Sensors/Actuators,” *ASME Journal of Applied Mechanics*, Vol. 57, pp. 434-441 (June 1990).
2. Enenkl, B., Kloppel, V., and Preibler, D., “Full Scale Rotor with Piezoelectric Actuatred Blade Flaps,” 28th European Rotorcraft Forum, Bristol, United Kingdom, 2002.
3. Samak, D. K., Chopra, I., “Design of High Force, High Displacement Actuators for Helicopter Rotors,” Smart Structures and Intelligent Systems; Proceedings of the Conference, Orlando, FL, Feb, 1994.
4. Kim, J.-S., Smith, E. C., and Wang, K. W., “Helicopter Vibration Suppression via Multiple Trailing Edge Flaps Controlled by Resonance Actuation System,” American Helicopter Society 60th Annual Forum, Baltimore Maryland, May 2004.
5. Lee, T.-O., and Chopra, I., “Design Issues of a High-Stroke, On-Blade Piezostack Actuator for a Helicopter Rotor with Trailing-Edge Flaps,” Journal of Intelligent Material Systems and Structures, Vol. 11, 2000, pp. 328-342.
6. Prechtl, E. F., and Hall, S. R., “X-Frame Actuator Servo-Flap Actuation System for Rotor Control,” SPIE: Smart Structures and Integrated Systems, San Diego CA, March 1998.
7. Jiang, J., and Mockensturm, E. M., “A Novel Motion Amplifier Using Axial Driven Buckling Beam,” 2003 ASME International Mechanical Engineering Congress, Washington DC, November 2003.
8. Bauchau, O. A., “Computational Schemes for Flexible, Nonlinear Multi-Body Systems,” Multibody System Dynamics, Vol. 2, 1998, pp. 169-225.
9. Hodges, D. H., “A mixed variational formulation based on exact intrinsic equations for dynamics of moving beams,” International Journal of Solids and Structures, Vol. 26, No.11, 1990, pp.1253-73.
10. Peters, D. A., and He, C. J., “Finite State Induced Flow Models Part II: Three Dimensional Rotor Disk,” Journal of Aircraft, Vol. 32, No 2, 1995, pp. 323-333.
11. Lake, R.C., Nixon, M.W., Wilbur, M.L., Singleton, J.D., and Mirick, P.H., “Demonstration of Passive Blade Twist Control Using Extension Twist Coupling,” NASA Tech Memo 107642/USAAVSCOM Tech Report 92-B-010, June 1992.
12. Wilbur, M. L., Mirick, P. H., Yeager, Jr. W. T., Langston, C. W., Cesnik, C. E. S., and Shin, S. -J., “Vibratory Loads Reduction Testing of the NASA/Army/MIT Active Twist Rotor,” Journal of the American Helicopter Society, Vol.47, No.2, 2002, pp.123-133.